SOFT ROBOTS

Bioinspired dual-stiffness origami

Stefano Mintchev[1], Jun Shintake[1,2], Dario Floreano[1]*

Origami manufacturing has led to considerable advances in the field of foldable structures with innovative applications in robotics, aerospace, and metamaterials. However, existing origami are either load-bearing structures that are prone to tear and fail if overloaded or resilient soft structures with limited load capability. In this manuscript, we describe an origami structure that displays both high load bearing and high resilience characteristics. The structure, which is inspired by insect wings, consists of a prestretched elastomeric membrane, akin to the soft resilin joints of insect wings, sandwiched between rigid tiles, akin to the rigid cuticles of insect wings. The dual-stiffness properties of the proposed structure are validated by using the origami as an element of a quadcopter frame that can withstand aerodynamic forces within its flight envelope but softens during collisions to avoid permanent damage. In addition, we demonstrate an origami gripper that can be used for rigid grasping but softens to avoid overloading of the manipulated objects.

INTRODUCTION

Folding has been typically investigated to make large structures easy to store and transport (*1*), but it holds the potential to improve the way we experience daily and personal technologies. For example, shape-shifting by folding is a promising strategy to tailor the morphology and mechanical properties of reconfigurable objects (*2*), reprogrammable metamaterials (*3*, *4*), and multimodal and crash-resilient robots (*5*, *6*). Folding is often leveraged by nature across very different space and time scales. Protein chains assume different biologically functional morphologies by folding (*2*), and many animals display foldable bodies to adapt their morphology when transitioning between different environments (*3*), to extend their flight envelope (*4*), to protect themselves from harsh environments or predators (*5*), to decrease their size when moving in confined space (*6*, *7*), and to mitigate the consequences of collisions (*8*).

Intrigued by such potential, engineers and roboticists have investigated different folding mechanisms and technologies to functionalize artificial systems. For instance, multijoint folding mechanisms are composed of rigid links connected through a variety of motor-actuated joints or springs (*9*). However, the resulting structures tend to be bulky, prone to failure during collisions, and difficult to scale. A different approach consists of using deformable elastic elements [e.g., thin shells of fiber composite materials (*10*)], which are simpler to manufacture, but have limited folding patterns because sharp folds are constrained by the strain limit of the materials. Other foldable structures, such as inflatable systems, can markedly reduce their size but require bulky and heavy pressurization systems for deployment (*11*).

Recent advances in origami technologies have led to a quantum leap in the field of foldable structures. Origami manufacturing is a promising method to embed complex folding patterns in lightweight structures with an easy, cost-effective, and scalable manufacturing process (*12*). Although origami structures have already found application in several fields, such as aerospace robotics (*13*), terrestrial robotics (*12*, *14*), aerial robotics (*15*–*17*), medical equipment (*18*, *19*), and packaging (*20*), they suffer from various shortcomings. Most origami structures are made of rigid laminated materials and rigid joints [i.e., inextensible joints made of polyimide or nylon (*21*)], which leads to limitations that are characteristic of intrinsically rigid systems. For instance, rigid origamis are fragile, are prone to tear (*22*), and easily fail when overloaded during collisions (*15*). Elastomer origamis (*23*–*25*) are more robust, adaptable, and safe, but their load-bearing capability is not comparable with that of rigid origamis and often requires pressurizing systems to withstand loads (*23*, *24*).

The challenge of strategically tailoring stiffness and softness of foldable structures is mastered by insects whose evolved origami wings are composed of rigid tiles of cuticle connected through soft resilin joints (Fig. 1A) (*26*). The coexistence of rigid and soft materials confers on the insect wing not only the compliance required to fold (*27*) and to survive collisions (*8*) but also the stiffness required to withstand 20 to 1000 beats per second during flight (*28*, *29*). Resilin is one of the most efficient elastic proteins known (*30*) and is located in strategic regions of the wing, most notably along the folds. Resilin works as a spring capable of storing and releasing mechanical energy for rapid wing folding or unfolding (*27*) and prevents fatigue during folding, greatly reducing wing wear (*27*). Furthermore, Mountcastle and Combes (*8*) found that resilin is responsible for the dual-stiffness behavior of wasp wings (e.g., the ability to reversibly transition between rigid and soft states), which provides mechanical resilience without impairing flight performances. For example, in the wings of yellowjackets (*Vespula maculifrons*), a resilin joint allows the wing tip to slightly flex during flight (rigid state) but reversibly crumple along the flexion line during collisions (soft state).

Recently, Faber *et al.* (*31*) presented a three-dimensional printing process for the development of bioinspired spring origamis that capture some of the properties that arise from the combination of soft joints and rigid tiles. Specifically, the possibility of broadening the folding design space and achieving a bistable behavior for rapid folding is described. Despite the self-locking capabilities of the bioinspired spring origami, the proposed manufacturing process of soft joints leads to structures that largely deform when loaded and limits their use when high load bearing is needed.

In this manuscript, we describe an origami design principle, which is inspired by insect wings, to address the challenges of achieving both high load bearing and resilience in folding structures. The design principle consists of an integrated structure composed of prestretched elastomeric membranes, akin to the insect resilin joints, sandwiched

[1]Institute of Microengineering, School of Engineering, École Polytechnique Fédérale de Lausanne, 1015 Lausanne, Switzerland. [2]Department of Mechanical and Intelligent Systems Engineering, School of Informatics and Engineering, University of Electro-Communications, Tokyo 182-8585, Japan.
*Corresponding author. Email: dario.floreano@epfl.ch

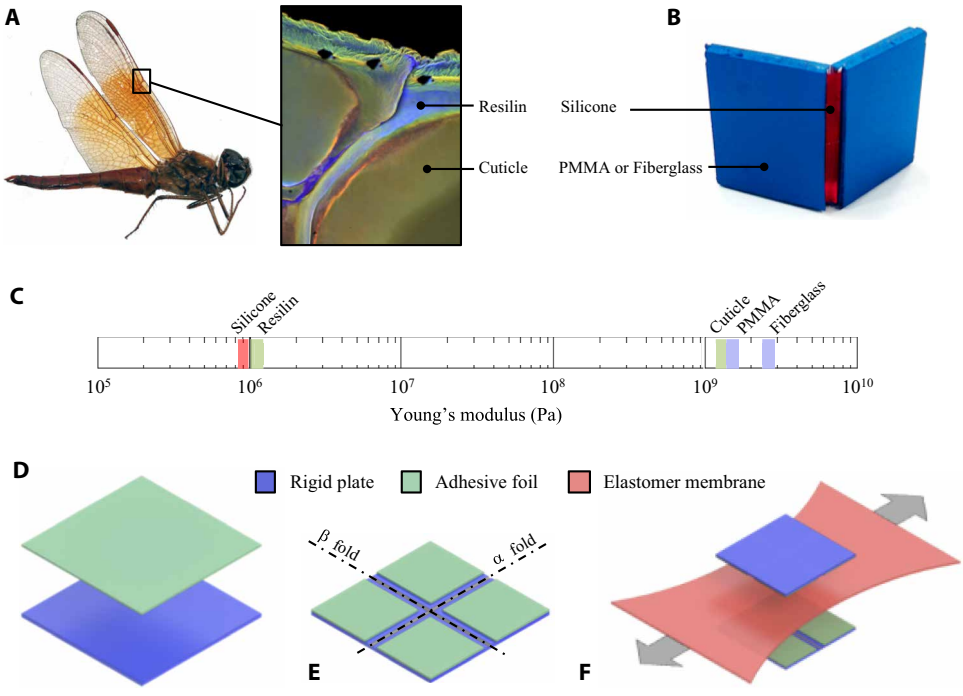

Fig. 1. Bioinspired dual-stiffness origami. (**A**) Pictures of a *Brachythemis contaminata* and of its hindwing nodus. Blue, green, and red indicate the presence of resilin, less-sclerotized cuticle, and highly sclerotized cuticle, respectively [images adapted from (*29*)]. (**B**) Structure of the bioinspired dual-stiffness origami consisting of prestretched elastomeric membranes, akin to resilin joints of insect wings, sandwiched between rigid tiles, akin to cuticles of insect wings. (**C**) Young's moduli of the elastomeric membrane and the rigid tiles are the same as those of resilin and cuticle. (**D**) The rigid plate and the adhesive foil are bonded together into a single composite structure. (**E**) The composite is laser-machined to engrave the folding pattern (here, two transversal folds) and to remove the adhesive foil along the folding pattern. (**F**) Two composite structures are bonded on a prestretched elastomer membrane.

between rigid tiles, akin to the insect cuticles (Fig. 1B). The elastomeric membrane and the rigid tiles that we used exhibit Young's moduli in the same range as those of resilin and cuticle (Fig. 1C). We validated this design principle in two robotic systems: (i) a foldable frame for a hovering drone, which can sustain the drone weight within its flight envelope, undergo large deformation when folding, buckle in collisions and prevent damage, and store energy that can be used for rapid self-deployment; and (ii) a gripper that can rigidly manipulate objects and buckle to avoid overloading of the objects. This design principle could find applications in a variety of areas, such as shape-shifting robots, mobile electronic devices, portable tools, antennas, and any other man-made structures that could benefit from resilient folding, compliance and robustness, and energy absorption.

RESULTS

Here, we describe a bioinspired strategy to abstract and translate insect wing key features—load bearing, energy storage, and resilience—into man-made thin folding structures. The method consists of joining rigid tiles (equivalent to biological cuticles) with prestretched elastomer membranes (equivalent to resilin) positioned at strategic locations of the structure (Fig. 1, D to F; see also movie S1). The elastomer membrane (e.g., silicone or latex) is prestretched and sandwiched between rigid tiles (e.g., acrylic or fiberglass). First, we assessed the mechanical properties of the origami structure using samples that have a single folding line. Second, we validated the design principle of dual-stiffness structures of a foldable quadcopter and of a robotic gripper with multiple folding lines.

Mechanical properties of the compliant origami

Figure 2A shows a simple compliant origami composed of a single fold perpendicular to the direction of the prestretch of the membrane. The membrane is made of the elastomer Nusil CF19-2186 with a thickness of 0.3 mm and a prestretch ratio of 2 and is bonded between two poly(methyl methacrylate) (PMMA) tiles with a thickness of 0.5 mm. The prestretched soft membrane confers a dual-stiffness behavior on the fold of the origami. Theoretically, the fold stretches axially only when the load overcomes a threshold defined by the initial prestretch of the membrane (Fig. 2B and the theoretical model in Supplementary Materials). Experimentally, the origami displays high stiffness for axial loads below the threshold and softens when the threshold is exceeded. For the same reason, the structure substantially folds only when the threshold is exceeded (Fig. 2C). In other words, the origami has a dual-stiffness behavior that conveniently merges the features of rigid and soft systems: load bearing in the stiff state and resilience and safe interaction in the soft state. Moreover, the membrane stretches during folding and stores elastic energy that can be used to rapidly deploy the compliant origami, and it can intrinsically accommodate the thickness of the tiles in folded state without resorting to dedicated methods that increase design and manufacturing complexity (*16*, *32*). For a given geometry of the fold and material of the membrane, the behavior of the dual-stiffness origami depends on two parameters. The prestretch value (λ) of the membrane affects the stiffness threshold, as shown in Fig. 2D. After the threshold, the length of the fold membrane that is not bonded to the tiles (L in Fig. 2A) affects the stiffness of the membrane, as shown in Fig. 2E. By varying these two parameters, the overall behavior of the dual-stiffness origami can be tuned for different applications (see also the theoretical model in the Supplementary Materials). Furthermore, similar to other origami manufacturing techniques, the design can be scaled to larger structures by stacking multiple layers of elastomer membranes and rigid tiles. A multilayer approach is also a viable solution to enable dual-stiffness behavior in joints that have different orientations. For example, with reference to Fig. 1E, a dual-stiffness behavior in the β fold can be achieved by adding a layer with a membrane prestretched perpendicularly to that fold. The same procedure can be repeated for each fold that is required to have dual stiffness in a different orientation.

Crash-resilient and self-deployable quadcopter

The compliant origami was applied to a pocket-sized quadcopter composed of four foldable arms that can be wrapped around the main

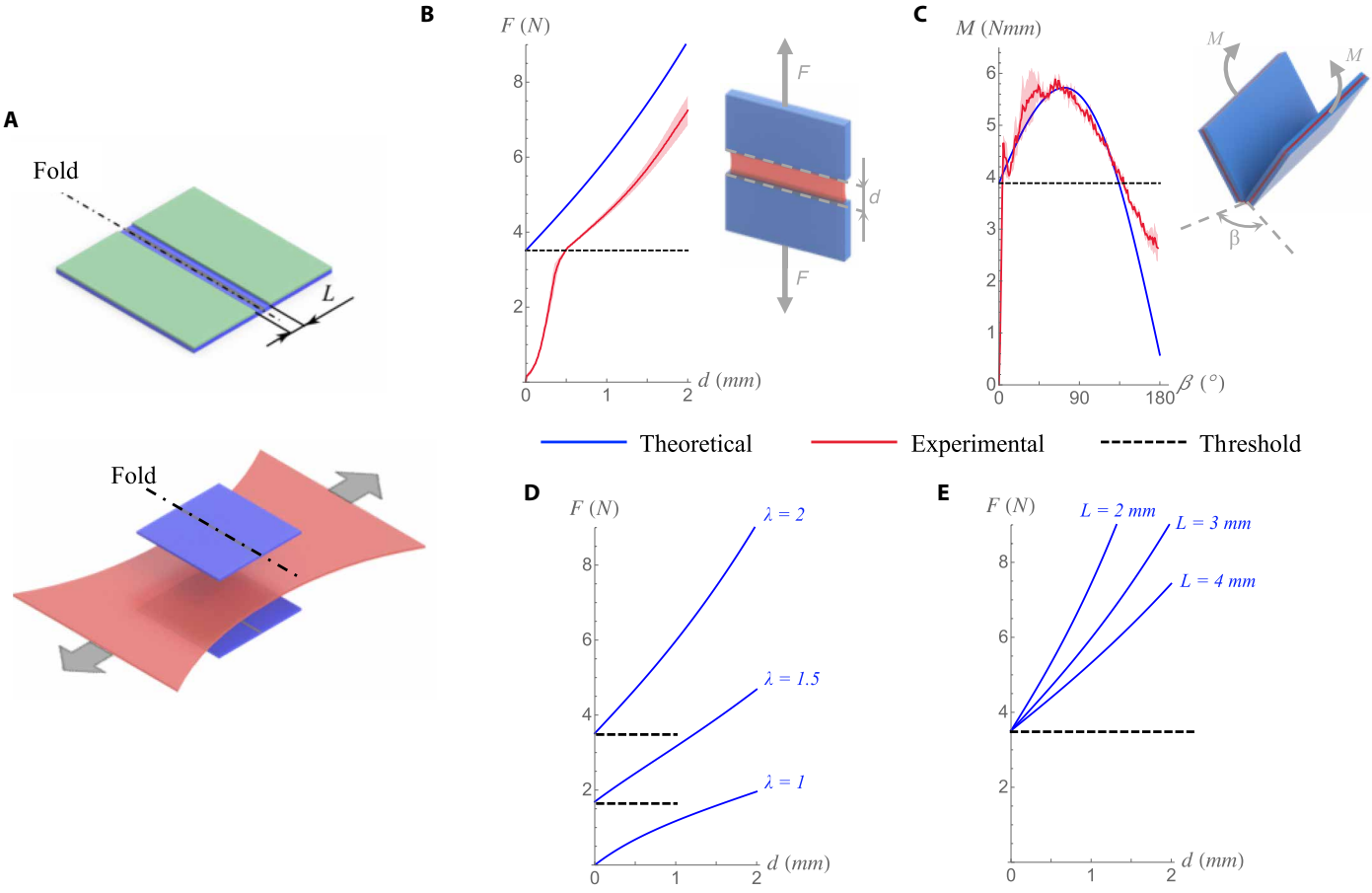

Fig. 2. Mechanical behavior. (**A**) The compliant origami consists of three layers: a prestretched elastomer membrane bonded between two outer tiles of rigid material. *L* is the length of the membrane around the fold that is not bonded to the rigid plate and, hence, is free to deform when the origami is stretched. (**B**) Under axial load *F*, the fold stretches only when the load exceeds a threshold indicated by the horizontal dashed line. (**C**) When folded with the bending angle β, the origami undergoes deflection upon exceeding the threshold of the moment *M* indicated by the horizontal dashed line. (**D**) The model predicts an increase in the transition threshold when the prestretch of the silicone membrane is increased. (**E**) The model predicts a decrease in the stiffness of the origami structure when the length *L* is increased.

frame during storage and transportation (Fig. 3A). The crease pattern of the arm comprised one longitudinal and two transversal folds. During flight, each arm assumed a deployed configuration with a triangle-shaped section constrained by resistive moments (M_{Res}), which were generated by two couples of magnets placed in the arm and frame (see partial section in Fig. 3A). Furthermore, the possibility to reversibly transition between rigid and soft states may be useful for frames and wings for drones that not only rigidly withstand flexural loads within a desired flight envelope but also fold to prevent damage when forces rapidly increase during collisions (*33*).

The flexural behavior of the arm is defined by the prestretched membrane and the specific crease pattern engraved in the arm (Fig. 3A), and it is essential for (i) withstanding loads within the flight envelope for maneuverable and stable flights, and (ii) deflecting and (iii) subsequently buckling to preserve structural integrity during collisions when the external load rapidly increases. This behavior is qualitatively illustrated in Fig. 3B, where the arm was subjected to a bending force, such as the thrust generated by propellers during flight. The origami structure displayed three phases as a function of the magnitude of the bending load: (i) the rigid phase, where the prestretch of the membrane constrained the deflection of the arm when the force was below a threshold, here set as 50% above the maximum thrust (T_{MAX}) generated by the propellers ($F < 1.5T_{MAX}$); (ii) the compliant phase, where the membrane further stretched when the flexural load was above the threshold ($F > 1.5T_{MAX}$); and (iii) the buckling phase, where the arm unfolded around the apex angle and offered low resistance to bending. The aforementioned phases are reflected in the flexural test of the arm (Fig. 3C). The trend measured in the experimental data is in agreement with the theoretical predictions of the model described in the Supplementary Materials. However, the theoretical model neglects shear deformations caused by the applied load and considers the apex angle unchanged until buckling, resulting in an overestimation of the force causing a deflection of the arm.

The mechanism eliciting buckling and its contribution to crash resilience is elucidated in Fig. 3 (D and E). When the membrane was further stretched in the compliant phase (Fig. 3B, phase ii), it generated a moment M_α that tends to unfold the arm around the apex angle. When this moment overcame the resistive moment of the magnets, M_{Res} (Fig. 3B), the arm buckled and unfolded around the apex angle. Just like in the wings of yellowjackets (*8*), this behavior is essential to preserve the integrity of the arm during collisions. When the arm buckled, the stress in the silicone membrane dropped without reaching the point

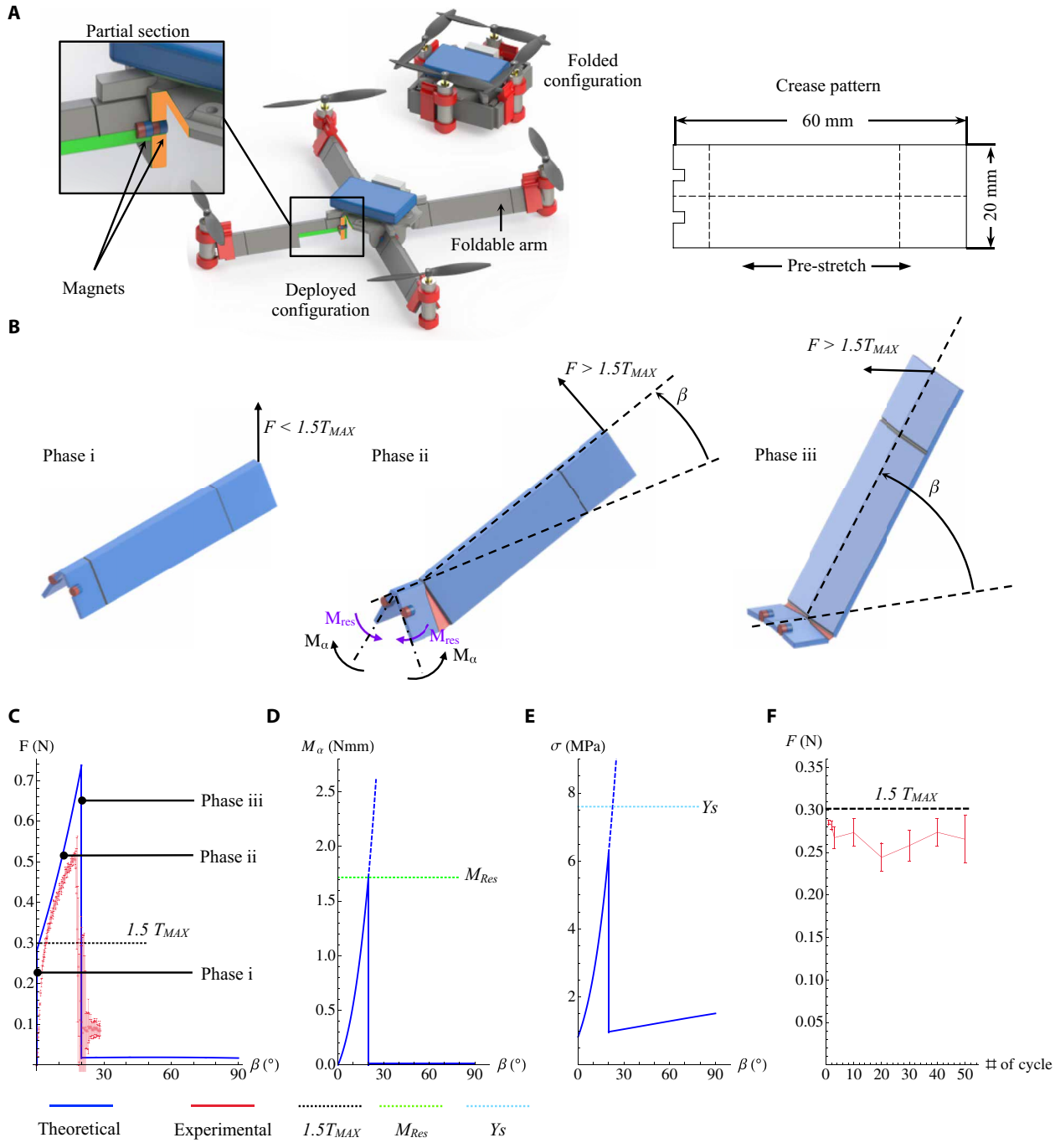

Fig. 3. Quadcopter equipped with dual-stiffness origami arms. (**A**) Three-dimensional model of the robot with a partial section highlighting the magnets that constrain the apex angle of the arm. The robot weighs 30 g and has a size of 160 mm by 160 mm by 30 mm when deployed and a size of 60 mm by 60 mm by 30 mm when folded. (**B**) The three phases of the arm behavior under flexural load. (**C**) Bending force *F*, (**D**) opening moment M_α, and (**E**) maximum stress σ in the silicone membrane as a function of the bending angle β. (**F**) Experimental data related to arm fatigue, force F_2 corresponding to a 2° deflection of the arm as a function of the number of cycles. The data summarize the results of fatigue tests on three arm samples. Error bars indicate SD.

of failure [Fig. 3E, yield strength (Y_s)] even when the arm underwent large deflections. The integrated silicone membrane conferred robustness on the origami arms, allowing multiple buckling cycles (e.g., due to folding or multiple collisions) without relevant effects on its load-bearing capabilities. As shown in Fig. 3C, even after 50 repeated cycles of buckling, the threshold force required to transition from the rigid phase (Fig. 3B, phase i) to the compliant phase (Fig. 3B, phase ii) remained constant. On the other hand, if the arm were not allowed to buckle, then the silicone membrane would fail after the first loading cycle, leading to a complete loss of load-bearing capability.

When the origami quadrotor flew against a wall (Fig. 4A; see also movie S2), the arms transitioned from a rigid state to a soft state and

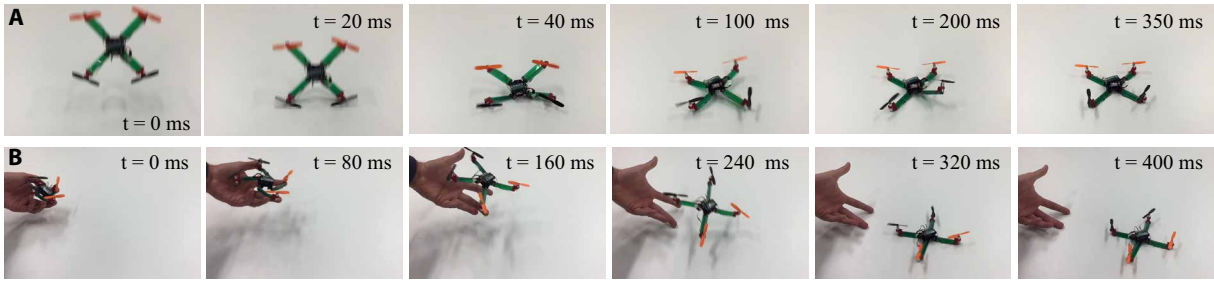

Fig. 4. Collision resilience and foldability of the origami drone. (**A**) Snapshots of a collision: The arms buckle and then go back to the initial flight configuration. (**B**) Snapshots of the deployment process: Initially, the arms are wrapped around the main frame and then self-deploy in the air using the energy stored in the elastomeric joints.

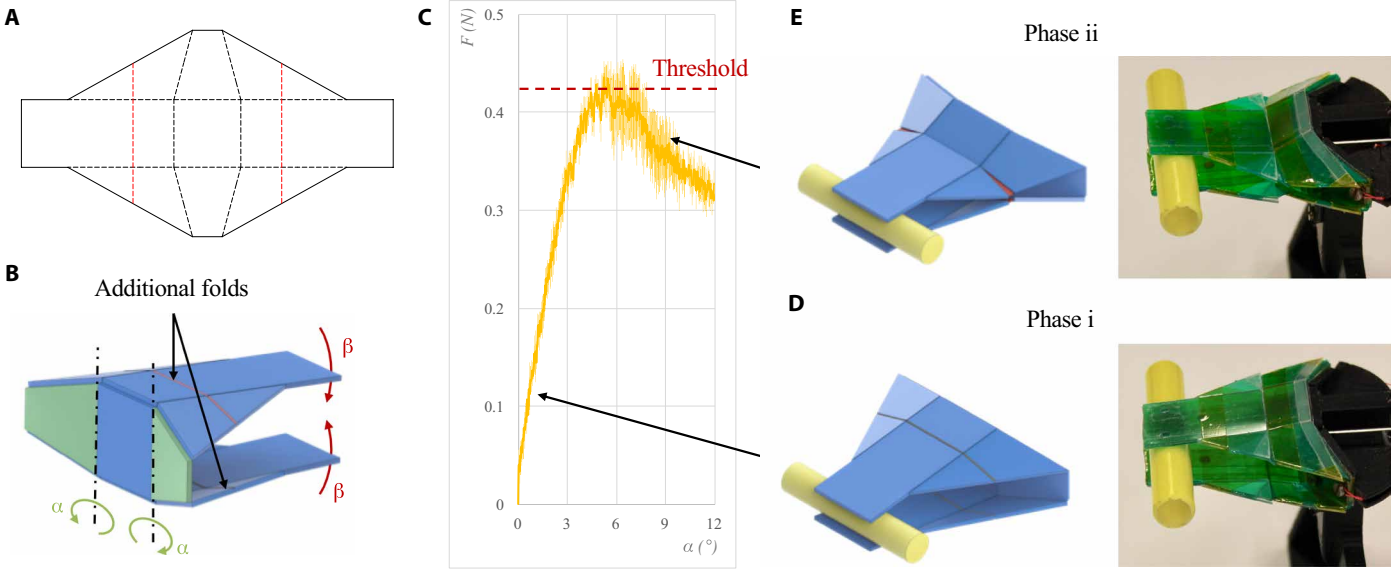

Fig. 5. Dual-stiffness origami gripper. (**A**) The original Oriceps (*18*) crease pattern was modified with two additional folds indicated by the red dashed lines. (**B**) The grasping motion of the compliant origami gripper (i.e., the bending angle β) is activated by folding the two input tiles highlighted in green with the angle α. (**C**) Experimental measurement of the grasping force *F* as a function of the input angle α. When the origami gripper grasps an object, the grasping force rapidly grows until a threshold is reached, as indicated by the horizontal dashed line, when the structure undergoes buckling along the compliant fold, hence avoiding overload of the grasped object. (**D**) The origami gripper in the rigid configuration firmly holding an object. (**E**) The origami gripper in the soft configuration holding an object without overloading it.

largely deformed without breaking; the arms subsequently redeployed with no permanent damage. This collision-resilient strategy was proposed by the authors with a previous origami design (*33*), which was very complex and required time-consuming assembly. The origami structure described here achieved similar performance with a scalable, rapid, and cost-effective manufacturing process. Furthermore, in addition to load bearing and crash resilience, the compliant origami also stored elastic energy that can be leveraged for self-deployment of the drone from a folded configuration. When the arms buckle due to a horizontal flexural load, the apex angle collapsed, and the arm can be wrapped around the main frame by folding along the transversal folds (Fig. 3A). During this process, the elastic membrane in the longitudinal joints stretched and stored energy that could be rapidly released to deploy the arms (Fig. 4B; see also movie S2).

Compliant origami gripper

Dual-stiffness behavior can also be useful for rigid grippers that soften to handle fragile objects (*34*). An origami gripper proposed in (*18*) was modified with two additional folds (Fig. 5A, red dashed lines) and manufactured using the method described above (see also movie S3). In folded configuration (Fig. 5B), the grasping motion (angle β) was obtained by folding together the two input tiles (angle α). Figure 5C shows the measured grasping force *F* as a function of the input angle α. The compliant origami can firmly hold an object and behave like a rigid gripper (Fig. 5D, phase i). However, when the gripping force exceeded the threshold, the origami behaved like a soft gripper and conformed to the object (Fig. 5E, phase ii), thus preventing overload without resorting to sensory feedback and active controllers. The force threshold causing the transition from rigid to soft can be changed by tuning the material properties of the membrane and the geometry of the folding pattern in the gripper. This behavior can be very useful for the precise and safe manipulation of fragile objects and living tissues. In addition, the simple and lightweight features and the relatively faster fabrication process of the compliant origami gripper make it advantageous in comparison with other soft grippers in the literature (*34*). However, the necessity of preprogramming the threshold force against a target object geometry may limit the size and types of objects that can be manipulated by a single compliant origami gripper.

DISCUSSION

Recent advances in origami technologies have led to a quantum leap in the field of foldable structures. However, rigid origamis are fragile, are prone to tear, and rapidly fail when overloaded during collisions. Instead, origamis with soft creases are more robust, adaptable, and safe, but their load-bearing capability is not comparable with that of rigid origamis. The proposed bioinspired origami structure combines the load-bearing capability of rigid material with the resilience, shape-shifting, and self-deployment capabilities of soft materials. The reversible stiffness change is encoded in the design of the origami and is triggered by external loads without the need of sensors and control. Although the mechanical behavior of single folds is explained by the proposed analytical model (see Supplementary Materials), the prediction of the behavior in complex folding structures would benefit from numerical modeling and computation tools specific for soft materials (*35*). Because the origami comprises elastomeric membranes, it is possible to envision a straightforward integration of soft actuators, such as dielectric polymer actuators, and of soft electronic circuitry (*36*, *37*). This could provide the origamis with controlled actuation and proprioception, thus opening new avenues for the development of multifunctional shape-shifting structures in robotics, aerospace, and consumer applications. For instance, compliant origamis could enable multifunctional wings for drones that can morph for efficient and maneuverable flight over a broad range of flight envelopes (*38*) and could embed distributed sensing (*39*) to perceive turbulences and improve flight stability (*40*).

MATERIALS AND METHODS

The fabrication process of the origami was based on conventional planar micromachining techniques (*12*), as illustrated in Fig. 1 and shown in movie S1. The process started with the fabrication of the elastomer membrane made of silicone rubber (Nusil CF19-2186). After mixing the two components of the elastomer per the manufacturer's recommendations, the silicone was blade-casted on a polyethylene terephthalate film by using a variable gap applicator (Zehntner ZUA2000) and a film applicator coater (Zehntner ZAA2300) and then cured in an oven for 60 min at 80°C. The desired thickness of the soft layer was achieved by the applicator gap. We used elastomer membranes with a thickness of 300 μm for all the prototypes. A PMMA plate and a silicone adhesive foil (Adhesives Research ARclear 8932EE) were bonded together (Fig. 1D). The composite structure was machined by using a CO_2 laser machine (Trotec Speedy 300). The laser works in three passes: A first low-power pass removes the adhesive foil along the folds, then a medium-power pass engraves the desired crease pattern in the PMMA plate, and, last, a high-power pass cuts the contour of the structure (Fig. 1E). The elastomer membrane was prestretched uniaxially with the desired ratio and mounted in a PMMA holding frame using the silicone adhesive foil. Two identical composite structures were attached on both sides of the membrane (Fig. 1F) and cut from the holding frame with scissors. Last, the PMMA plate was manually folded and broken along the engraved creases, while the elastomer membrane kept the multiple tiles of the structure together and resulted in the desired origami.

SUPPLEMENTARY MATERIALS

robotics.sciencemag.org/cgi/content/full/3/20/eaau0275/DC1
Supplementary Text
Fig. S1. Folding behavior of the dual-stiffness origami.
Fig. S2. Bending behavior of the dual-stiffness origami arm.
Table S1. Design parameters of the experimental sample.
Movie S1. Manufacturing process.
Movie S2. Crash-resilient and self-deployable quadcopter.
Movie S3. Compliant origami gripper.
References (*41*, *42*)

REFERENCES AND NOTES

1. S. Pellegrino, Deployable structures in engineering BT - Deployable structures, in *Deployable Structures* (Springer, 2001), pp. 1–35.
2. C. M. Dobson, Protein folding and misfolding. *Nature* **426**, 884–890 (2003).
3. D. K. Riskin, J. W. Hermanson, Biomechanics: Independent evolution of running in vampire bats. *Nature* **434**, 292 (2005).
4. D. Lentink, U. K. Müller, E. J. Stamhuis, R. de Kat, W. van Gestel, L. L. M. Veldhuis, P. Henningsson, A. Hedenström, J. J. Videler, J. L. van Leeuwen, How swifts control their glide performance with morphing wings. *Nature* **446**, 1082–1085 (2007).
5. J. T. Smigel, A. G. Gibbs, Conglobation in the pill bug, *Armadillidium vulgare*, as a water conservation mechanism. *J. Insect Sci.* **8**, 1–9 (2008).
6. K. Jayaram, R. J. Full, Cockroaches traverse crevices, crawl rapidly in confined spaces, and inspire a soft, legged robot. *Proc. Natl. Acad. Sci. U.S.A.* **113**, E950–E957 (2016).
7. C. D. Williams, A. A. Biewener, Pigeons trade efficiency for stability in response to level of challenge during confined flight. *Proc. Natl. Acad. Sci. U.S.A.* **112**, 3392–3396 (2015).
8. A. M. Mountcastle, S. A. Combes, Biomechanical strategies for mitigating collision damage in insect wings: Structural design versus embedded elastic materials. *J. Exp. Biol.* **217**, 1108–1115 (2014).
9. N. De Temmerman, C. A. Brebbia, *Mobile and Rapidly Assembled Structures IV: Computational Mechanics* (WIT Press, 2014).
10. H. M. Y. C. Mallikarachchi, S. Pellegrino, Design and validation of thin-walled composite deployable booms with tape-spring hinges, in *52nd AIAA/ASME/ASCE/AHS/ASC Structures, Structural Dynamics and Materials Conference 19th AIAA/ASME/AHS Adaptive Structures Conference 13t.* (American Institute of Aeronautics and Astronautics, 2011), pp. 1–17.
11. D. Cadogan, T. Smith, F. Uhelsky, M. Mackusick, Morphing inflatable wing development for compact package unmanned aerial vehicles, in *45th AIAA/ASME/ASCE/AHS/ASC Structures, Structural Dynamics and Materials Conference* (American Institute of Aeronautics and Astronautics, 2004).
12. S. Felton, M. Tolley, E. Demaine, D. Rus, R. Wood, A method for building self-folding machines. *Science* **345**, 644–646 (2014).
13. S. A. Zirbel, R. J. Lang, M. W. Thomson, D. A. Sigel, P. E. Walkemeyer, B. P. Trease, S. P. Magleby, L. L. Howell, Accommodating thickness in origami-based deployable arrays. *J. Mech. Des.* **135**, 111005 (2013).
14. A. Rafsanjani, Y. Zhang, B. Liu, S. M. Rubinstein, K. Bertoldi, Kirigami skins make a simple soft actuator crawl. *Sci. Robot.* **3**, eaar7555 (2018).
15. S. Mintchev, L. Daler, G. L'Eplattenier, L. Saint-Raymond, D. Floreano, Foldable and self-deployable pocket sized quadrotor, in *Proceedings - IEEE International Conference on Robotics and Automation* (IEEE, 2015), vol. 2015, pp. 2190–2195.
16. L. Dufour, K. Owen, S. Mintchev, D. Floreano, A drone with insect-inspired folding wings, in *IEEE International Conference on Intelligent Robots and Systems* (IEEE, 2016), vol. 2016, pp. 1576–1581.
17. S. J. Kim, D. Y. Lee, G. P. Jung, K. J. Cho , An origami-inspired, self-locking robotic arm that can be folded flat. *Sci. Robot.* **3**, eaar2915 (2018).
18. B. J. Edmondson, L. A. Bowen, C. L. Grames, S. P. Magleby, L. L. Howell, T. C. Bateman, Oriceps: Origami-inspired forceps, in *ASME 2013 Conference on Smart Materials, Adaptive Structures and Intelligent Systems* (ASME, 2013), pp. V001T01A027.
19. T. G. Nelson, R. J. Lang, S. P. Magleby, L. L. Howell, Curved-folding-inspired deployable compliant rolling-contact element (D-CORE). *Mech. Mach. Theory* **96**, 225–238 (2016).
20. S. S. Tolman, I. L. Delimont, L. L. Howell, D. T. Fullwood, Material selection for elastic energy absorption in origami-inspired compliant corrugations. *Smart Mater. Struct.* **23**, 094010 (2014).
21. H. McClintock, F. Z. Temel, N. Doshi, J. S. Koh, R. J. Wood, The milliDelta: A high-bandwidth, high- precision, millimeter-scale Delta robot. *Sci. Robot.* **3**, eaar3018 (2018).
22. D. W. Haldane, R. S. Fearing, Running beyond the bio-inspired regime, in *Proceedings - IEEE International Conference on Robotics and Automation* (IEEE, 2015), vol. 2015, pp. 4539–4546.
23. R. V. Martinez, C. R. Fish, X. Chen, G. M. Whitesides, Elastomeric origami: Programmable paper-elastomer composites as pneumatic actuators. *Adv. Funct. Mater.* **22**, 1376–1384 (2012).
24. S. Daynes, R. S. Trask, P. M. Weaver, Bio-inspired structural bistability employing elastomeric origami for morphing applications. *Smart Mater. Struct.* **23**, 125011 (2014).
25. B. H. Hanna, J. M. Lund, R. J. Lang, S. P. Magleby, L. L. Howell, Waterbomb base: A symmetric single-vertex bistable origami mechanism. *Smart Mater. Struct.* **23**, 094009 (2014).

26. R. J. Wootton, Functional morphology of insect wings. *Annu. Rev. Entomol.* **37**, 113–140 (1992).
27. F. Haas, S. Gorb, R. J. Wootton, Elastic joints in dermapteran hind wings: Materials and wing folding. *Arthropod Struct. Dev.* **29**, 137–146 (2000).
28. K. Saito, S. Yamamoto, M. Maruyama, Y. Okabe, Asymmetric hindwing foldings in rove beetles. *Proc. Natl. Acad. Sci. U.S.A.* **111**, 16349–16352 (2014).
29. H. Rajabi, N. Ghoroubi, K. Stamm, E. Appel, S. N. Gorb, Dragonfly wing nodus: A one-way hinge contributing to the asymmetric wing deformation. *Acta Biomater.* **60**, 330–338 (2017).
30. C. M. Elvin, A. G. Carr, M. G. Huson, J. M. Maxwell, R. D. Pearson, T. Vuocolo, N. E. Liyou, D. C. C. Wong, D. J. Merritt, N. E. Dixon, Synthesis and properties of crosslinked recombinant pro-resilin. *Nature* **437**, 999–1002 (2005).
31. J. A. Faber, A. F. Arrieta, A. R. Studart, Bioinspired spring origami. *Science* **359**, 1386–1391 (2018).
32. R. J. Lang, K. A. Tolman, E. B. Crampton, S. P. Magleby, L. L. Howell, A review of thickness-accommodation techniques in origami-inspired engineering. *Appl. Mech. Rev.* **70**, 010805 (2018).
33. S. Mintchev, S. de Rivaz, D. Floreano, Insect-inspired mechanical resilience for multicopters. *IEEE Robot. Autom. Lett.* **2**, 1248–1255 (2017).
34. J. Shintake, V. Cacucciolo, D. Floreano, H. Shea, Soft robotic grippers. *Adv. Mater.* **7**, 1707035 (2018).
35. X. Zhao, Z. Suo, Method to analyze programmable deformation of dielectric elastomer layers. *Appl. Phys. Lett.* **93**, 251902 (2008).
36. S. Bauer, S. Bauer-Gogonea, I. Graz, M. Kaltenbrunner, C. Keplinger, R. Schwödiauer, 25th anniversary article: A soft future: From robots and sensor skin to energy harvesters. *Adv. Mater.* **26**, 149–161 (2014).
37. L. Hines, K. Petersen, G. Z. Lum, M. Sitti, Soft actuators for small-scale robotics. *Adv. Mater.* **29**, 1603483 (2017).
38. S. Barbarino, O. Bilgen, R. M. Ajaj, M. I. Friswell, D. J. Inman, A review of morphing aircraft. *J. Intell. Mater. Syst. Struct.* **22**, 823–877 (2011).
39. A. Mohamed, S. Watkins, R. Clothier, M. Abdulrahim, K. Massey, R. Sabatini, Fixed-wing MAV attitude stability in atmospheric turbulence—Part 2: Investigating biologically-inspired sensors. *Prog. Aerosp. Sci.* **71**, 1–13 (2014).
40. A. Mohamed, M. Abdulrahim, S. Watkins, R. Clothier, Development and flight testing of a turbulence mitigation system for micro air vehicles. *J. Field Robot.* **33**, 639–660 (2016).
41. O. H. Yeoh, Some forms of the strain energy function for rubber. *Rubber Chem. Technol.* **66**, 754–771 (1993).
42. J. Shintake, S. Rosset, B. E. Schubert, D. Floreano, H. R. Shea, A foldable antagonistic actuator. *IEEE/ASME Trans. Mechatron.* **20**, 1997–2008 (2015).

Funding: This study was supported by the Swiss National Science Foundation through the National Center of Competence in Research Robotics. **Author contributions:** S.M., J.S., and D.F. developed the concept and wrote the manuscript. S.M. and J.S. fabricated the experimental samples of the compliant origami, the quadcopter, and the soft gripper. S.M. designed the experiments and performed characterization of the experimental samples, the quadcopter, and the soft gripper. **Competing interests:** The authors declare that they have no competing financial interests. **Data and materials availability:** All data needed to evaluate the study are presented in the main text or the Supplementary Materials. The experimental data are available at Zenodo (DOI: 10.5281/zenodo.1287899). Contact S.M. for other materials.

Submitted 30 April 2018
Accepted 9 July 2018
Published 25 July 2018
10.1126/scirobotics.aau0275

Citation: S. Mintchev, J. Shintake, D. Floreano, Bioinspired dual-stiffness origami. *Sci. Robot.* **3**, eaau0275 (2018).

Bioinspired dual-stiffness origami

Stefano Mintchev, Jun Shintake and Dario Floreano

Sci. Robotics **3**, eaau0275.
DOI: 10.1126/scirobotics.aau0275